

Enhancing the Goos-Hänchen shift based on quasi-bound states in the continuum through material asymmetric dielectric compound gratings

Xiaowei Jiang(江孝伟), Bin Fang(方彬), and Chunlian Zhan(占春连)

Citation: Chin. Phys. B, 2024, 33 (**3**): 034206. DOI: 10.1088/1674-1056/acf661
Journal homepage: http://cpb.iphy.ac.cn; http://iopscience.iop.org/cpb

What follows is a list of articles you may be interested in

Multi-channel generation of vortex beams with controllable polarization states and orbital angular momentum

Ziyao Lyu(吕子瑶), Pan Wang(王潘), and Changshun Wang(王长顺)
Chin. Phys. B, 2023, 32 (**12**): 124209. DOI: 10.1088/1674-1056/ace767

Bound states in the continuum in metal—dielectric photonic crystal with a birefringent defect

Hongzhen Tang(唐宏珍), Peng Hu(胡鹏), Da-Jian Cui(崔大健), Hong Xiang(向红), and Dezhuan Han(韩德专)
Chin. Phys. B, 2022, 31 (**10**): 104209. DOI: 10.1088/1674-1056/ac6db6

Brightening single-photon emitters by combining an ultrathin metallic antenna and a silicon quasi-BIC antenna

Shangtong Jia(贾尚曈), Zhi Li(李智), and Jianjun Chen(陈建军)
Chin. Phys. B, 2022, 31 (**1**): 014209. DOI: 10.1088/1674-1056/ac248c

Dynamic shaping of vectorial optical fields based on two-dimensional blazed holographic grating

Xinyi Wang(王心怡), Yuan Gao(高源), Zhaozhong Chen(陈召忠), Jianping Ding(丁剑平), Hui-Tian Wang(王慧田)
Chin. Phys. B, 2020, 29 (**1**): 014208. DOI: 10.1088/1674-1056/ab5a3b

Design of an augmented reality display based on polarization grating

Renjie Xia(夏人杰), Changshun Wang(王长顺), Yujia Pan(潘雨佳), Tianyu Chen(陈天宇), Ziyao Lyu(吕子瑶), Lili Sun(孙丽丽)
Chin. Phys. B, 2019, 28 (**7**): 074201. DOI: 10.1088/1674-1056/28/7/074201

Enhancing the Goos–Hänchen shift based on quasi-bound states in the continuum through material asymmetric dielectric compound gratings

Xiaowei Jiang(江孝伟)[1,2], Bin Fang(方彬)[1,†], and Chunlian Zhan(占春连)[1,‡]

[1] *College of Optical and Electronic Technology, China Jiliang University, Hangzhou* 310018, *China*
[2] *College of Information Engineering, Quzhou College of Technology, Quzhou* 324000, *China*

(Received 11 July 2023; revised manuscript received 18 August 2023; accepted manuscript online 4 September 2023)

Quasi-bound state in the continuum (QBIC) resonance is gradually attracting attention and being applied in Goos–Hänchen (GH) shift enhancement due to its high quality (Q) factor and superior optical confinement. Currently, symmetry-protected QBIC resonance is often achieved by breaking the geometric symmetry, but few cases are achieved by breaking the material symmetry. This paper proposes a dielectric compound grating to achieve a high Q factor and high-reflection symmetry-protectede QBIC resonance based on material asymmetry. Theoretical calculations show that the symmetry-protected QBIC resonance achieved by material asymmetry can significantly increase the GH shift up to −980 times the resonance wavelength, and the maximum GH shift is located at the reflection peak with unity reflectance. This paper provides a theoretical basis for designing and fabricating high-performance GH shift tunable metasurfaces/dielectric gratings in the future.

Keywords: bound state in the continuum, Goos–Hänchen shift, dielectric compound grating, material asymmetry

PACS: 42.40.Eq, 42.79.Fm, 78.67.Pt **DOI:** 10.1088/1674-1056/acf661

1. Introduction

The interaction between light and matter has always been the core of nanophotonics research.[1,2] Realizing light localization in subwavelength structures with ultra-long radiation lifetimes is crucial for applications such as lasers, modulators, nonlinear optics and quantum computing.[3–7] Therefore, the bound states in the continuum (BICs) with infinite quality (Q) factor and superior light confining ability have aroused great interest. BIC is a ubiquitous physical phenomenon that was originally proposed in hypothetical quantum structures by Neumann and Wigner.[8] BIC is a local state that coexists with the continuum spectrum, is found in many physical structures, such as gratings or metasurfaces,[9–12] and has been used to realize interesting physical phenomena such as high Q near perfect absorption resonance with unpolarized focused light[13] and Goos–Hänchen (GH) shift enhancement.[14,15] However, BIC is a dark mode with an invisible scattering spectrum,[16] which makes it impossible to detect in practice. By breaking the symmetry of the metasurface or grating to transform the BIC into a symmetry-protected quasi-BIC (QuasiBIC, QBIC) with a finite but extremely high Q factor and an ultra-narrow linewidth,[17,18] QBIC can be detected in the form of Fano resonance.

Two common methods to break the plane symmetry of a grating or metasurface are to change the geometry of the grating or metasurface unit[17–19] and to change the refractive index of the grating or metasurface unit material.[20–23] Most of the current studies are based on geometric asymmetry to achieve symmetry-protected QBIC resonance, but this approach suffers from the problem of imposing fundamental limitations on achieving the lowest geometric asymmetry, especially in the near-infrared and visible spectral bands.[23] The Q factor is directly proportional to the negative quadratic of the asymmetry of the structure.[17–19] Therefore, the Q factor will significantly vary with the change in structural asymmetry, but there may be errors in the fabrication process, resulting in poor controllability.[19] Compared with geometric asymmetries, material asymmetry has the advantage of abundant means of implementation, such as by current injection,[24] photothermal effect,[25] Kerr effect[26] and epitaxy.[22] In addition, the material asymmetric grating or metasurface has strong controllability. Currently, there is not much research on material asymmetry in metasurfaces or gratings. Thus, we believe that the field requires further exploration in structural design and physical analysis.

Since it was first theoretically and experimentally demonstrated,[27] the GH effect has attracted attention as one of the important physical optics phenomena due to its profound physical significance and broad application scenarios.[28,29] The GH effect shows that when a beam of light is incident at the interface of two media and is totally reflected, the reflected beam will be laterally shifted relative to the path predicted by geometrical optics.[30,31] This lateral shift is called the GH shift. According to the stationary phase

†Corresponding author. E-mail: binfang@cjlu.edu.cn
‡Corresponding author. E-mail: zc913@163.com

© 2024 Chinese Physical Society and IOP Publishing Ltd

method,[32] the GH shift is proportional to the partial derivative of the reflection phase to the incident angle. Therefore, the GH shift can be enhanced through high Q factor resonance because the reflection phase will dramatically vary around the resonant angle.[14,15] Currently, different methods have been proposed to achieve high Q factor resonance, all of which significantly improve the GH shift, but their maximum GH shift is located at the reflectance dip.[33–36] In these studies, the reflectivity that corresponds to the maximum GH shift is even less than 0.1%, which is not conducive to the detection of GH shift signals in practical applications.

In recent years, it has been found that by using QBIC resonance, the GH shift can be enhanced, and the maximum GH shift can be guaranteed to be located at the reflection peak with perfect reflection. Zhang,[37] Wu[14,15] and Huang[38] used QBIC resonance to significantly enhance the GH shift in the near-infrared and terahertz bands, and the maximum GH shift was located at the reflection peak with unity reflectance. The QBIC resonance to enhance the GH shift in the aforementioned studies was achieved through geometric asymmetry. There are few studies based on material asymmetry to achieve QBIC resonance and even fewer studies based on material asymmetry to achieve GH shift enhancement. Although Berte,[20] Liu,[21] Yu,[22] Chen[23] and some others realized symmetry-protected QBIC resonance based on material asymmetry, none of them applied QBIC in GH shift enhancement.

In this paper, we propose to achieve QBIC resonance through dielectric compound grating with material asymmetry and enhance the GH shift by QBIC with the maximum GH shift at the reflectance peak. The effect of the grating structural parameters and material asymmetry on the QBIC resonance wavelength and linewidth is analyzed in detail. Theoretical calculations show that the GH shift can reach −980 times the resonance wavelength, and the effect of the grating structural parameters on the GH shift is investigated. The sensitivity of the grating as a refractive index sensor is calculated to be 1.96×10^6 μm/refractive index unit (RIU). This study can provide a theoretical basis for the design and fabrication of GH shift tunable metasurfaces or gratings in the future.

2. Structural design and calculation methods

Figure 1(a) shows a three-dimensional schematic of the dielectric compound grating. In the figure, the dielectric grating consists of a silicon dioxide (refractive index $n_s = 1.45$) substrate, a silicon (refractive index $n_{si} = 3.45$) waveguide layer and a compound grating layer. Within a grating period P, there are two gratings with different refractive indices, one composed of silicon and the other composed of a material with refractive index n. The material asymmetry parameter is $\gamma = n - n_{si}$. When an incident light (electric field linearly polarized along the y-axis direction) is obliquely incident to the dielectric grating along the z-axis at an angle of incidence θ, it is shifted by a distance along the x-axis direction (GH shift) and reflected to the free space at an angle of reflection θ. In Fig. 1(a), the GH shift can be divided into positive and negative GH shifts. Because the material asymmetry can excite the reflection QBIC resonance, it causes dramatic variation in the reflection phase around incident angle θ, which enhances the GH shift. Figure 1(b) shows specific parameters of the dielectric compound grating. The dielectric grating substrate thickness is $h_s = 220$ nm, the waveguide layer thickness is $h_w = 260$ nm, the grating thickness is $h_g = 160$ nm and the width and spacing of the two gratings in a single unit are w and $l = 400$ nm, respectively. Based on the above structural parameters, the QBIC resonance wavelength of the dielectric compound grating is around 1330 nm, this wavelength is useful in fields such as optical fiber communication and infrared night vision. Therefore, the dielectric compound grating that can achieve GH shift enhancement would be suitable for use as an optical device in optical fiber communication, infrared night vision, gas sensing and other related fields.

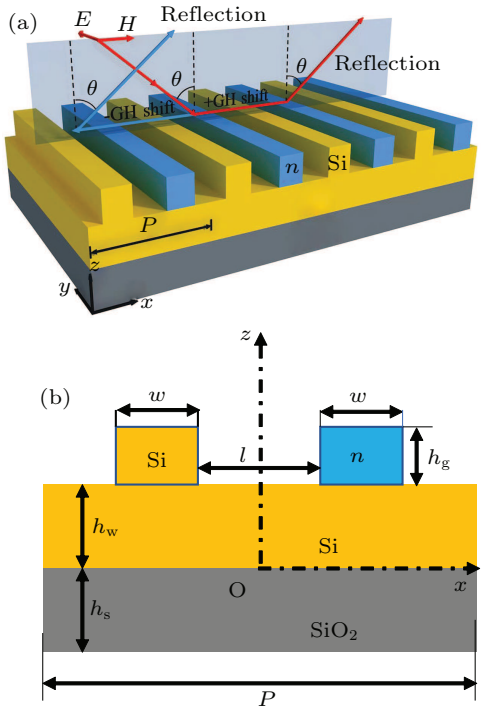


Fig. 1. Schematic illustration of the dielectric compound grating. (a) Three-dimensional schematic of the dielectric compound grating; (b) cross-section of the dielectric compound grating.

The proposed asymmetric dielectric compound gratings in this paper can be fabricated using existing semiconductor fabrication technology.[19,21] First, a layer of silicon is deposited on the silica substrate by plasma-enhanced chemical vapor deposition (PECVD), and the required silicon grating is obtained through electron beam lithography (EBL) and reactive ion etching (RIE). Second, a dielectric layer with refractive index n is deposited via epitaxial technique, followed by EBL and RIE, and a grating with refractive index n can be obtained. Finally, the protective layer on the grating is removed

by wet-etching to obtain the desired material asymmetric dielectric compound grating.

The permittivity of the grating layer can be expressed as[15,39]

$$\varepsilon(x) = \sum_m \varepsilon_m \exp\left(\mathrm{i}\frac{2m\pi x}{P}\right), \tag{1}$$

where ε_m is the grating Fourier harmonics and m is the order of the Fourier series. The grating Fourier harmonics can be expressed as

$$\varepsilon_0 = \frac{w}{P}n_{\mathrm{si}}^2 + \frac{w}{P}n^2 + \left(1-2\frac{w}{P}\right)n_{\mathrm{air}}^2 \quad (m=0), \tag{2}$$

$$\begin{aligned}\varepsilon_m = {} & \frac{\mathrm{i}}{2m\pi}\left\{(n_{\mathrm{si}}^2 - n_{\mathrm{air}}^2)\left[\exp\left(\mathrm{i}m\pi\frac{l}{P}\right)\right.\right. \\ & \left. - \exp\left(\mathrm{i}m\pi\frac{l}{P}\right)\exp\left(\mathrm{i}m\pi\frac{2w}{P}\right)\right] \\ & + (n^2 - n_{\mathrm{air}}^2)\left[\exp\left(\mathrm{i}m\pi\frac{-l}{P}\right)\exp\left(\mathrm{i}m\pi\frac{-2w}{P}\right)\right. \\ & \left.\left. - \exp\left(\mathrm{i}m\pi\frac{-l}{P}\right)\right]\right\} \quad (m\neq 0), \end{aligned} \tag{3}$$

where $n_{\mathrm{air}} = 1$. From Eqs. (1)–(3), the choice of refractive index n of the dielectric compound grating and the variation of the grating parameters will affect the dielectric compound grating permittivity.

The numerical theoretical calculation method in this paper is finite-difference time-domain (FDTD). To facilitate the calculation, we consider that the grating length along the y-axis is sufficiently long so that this paper calculates the two-dimensional dielectric compound grating based on FDTD. Because the incident light is obliquely incident to the dielectric grating at an angle of incidence θ, Bloch boundary conditions are added in the x-axis direction, while the perfect matching-layer boundary conditions are added in the z-axis direction.

3. Results and discussion

3.1. Symmetry-protected QBIC resonance excited by material asymmetry

To demonstrate that the symmetry-protected QBIC resonance can be excited by the material asymmetry, we calculated the reflection spectra of dielectric compound gratings with different material asymmetry parameters γ, as shown in Fig. 2. Currently, the incident angle $\theta = 6°$, $w = 200$ nm and $P = 1200$ nm. Figure 2(a) shows that when $\gamma = 0$, there is no resonance in the reflection spectra, but when $\gamma \neq 0$, there is a clear Fano resonance. As γ gradually moves away from 0, the resonance wavelength will blueshift ($\gamma < 0$) or redshift ($\gamma > 0$), and the resonance linewidth gradually widens. The reason is that γ affects the effective refractive index of the dielectric compound grating, and the resonance wavelength is related to the grating effective refractive index, as shown in Eq. (6). To make more intuitive observations, we show the resonance spectra in Fig. 2(b), where γ is -0.05, -0.15 and -0.25. As shown in Fig. 2(b), all cases achieve perfect reflection, the resonance linewidth widens and the resonance wavelength shows a blueshift when γ decreases. This phenomenon and the references[9–11,17,40] can prove that the resonance at $\gamma \neq 0$ is a QBIC resonance and is derived from the symmetry-protected BIC transformation.

In Fig. 2(a), identical absolute values of $\pm\gamma$ correspond to different grating resonance reflection spectra. To better understand the demonstration in Fig. 2(a), we show the reflection spectra of dielectric compound gratings, where γ is -0.15 and 0.15, in Fig. 2(c). Figure 2(c) shows that their reflection resonance wavelengths are not identical. Although $\gamma = -0.15$ and $\gamma = 0.15$ have identical absolute values, different refractive indices n can lead to different refractive indices of the dielectric compound grating, which affects the resonance wavelength of the grating.

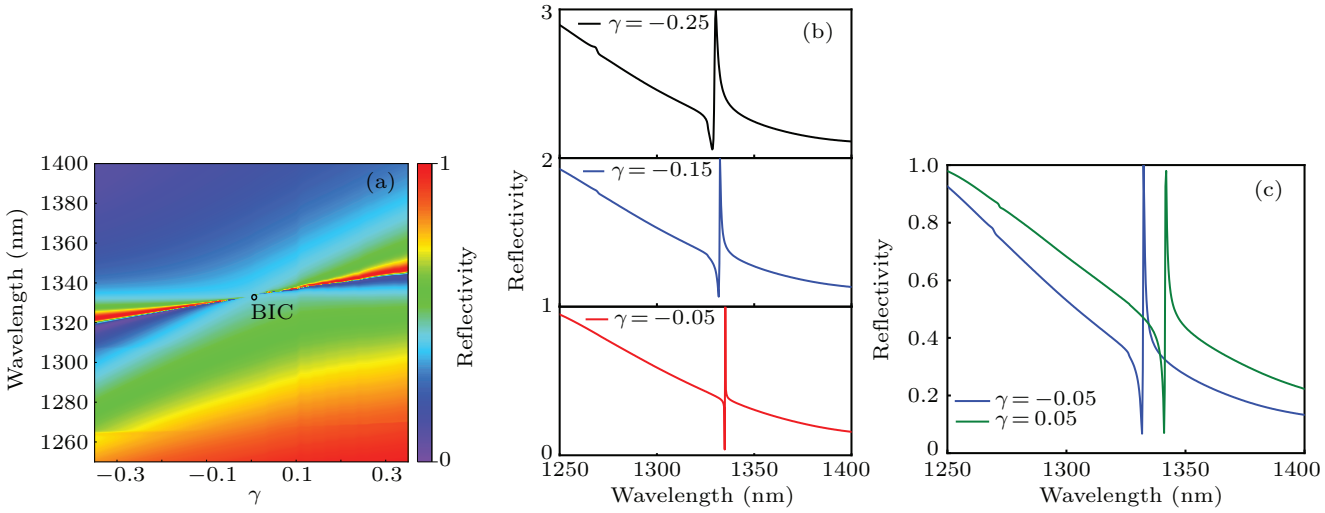


Fig. 2. Effect of asymmetric parameter γ on the grating reflection spectra. (a) Two-dimensional reflection spectra; (b) reflection spectra with γ being -0.05, -0.15 and -0.25; (c) reflection spectra with γ being -0.15 and 0.15.

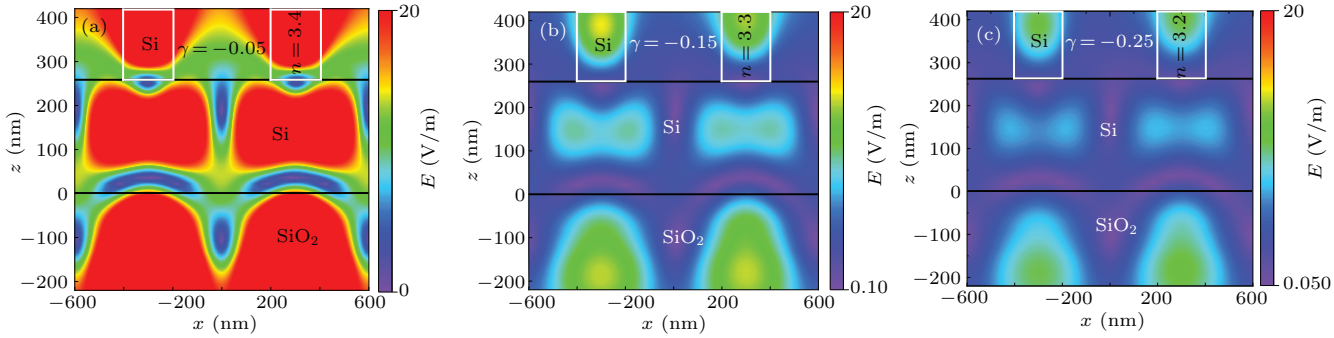


Fig. 3. Electric field distribution of the dielectric compound grating at the resonant wavelength with different values of material asymmetry parameter γ. (a) $\gamma = -0.05$; (b) $\gamma = -0.15$; (c) $\gamma = -0.25$.

There is no resonance in the dielectric compound grating at $\gamma = 0$ because the grating is symmetric in this case, the radiation channels between the grating and the free space are closed, and no energy can leak from the dielectric compound grating into free space. When $\gamma \neq 0$, i.e., the grating symmetry is broken and the radiation channels are formed, there is an energy leak from the grating into free space, and Fano resonances occur.[17,41,42] As γ gradually deviates from 0, which indicates that the asymmetry of the grating increases, more energy leaks into free space through the radiation channels.[17,41] Figure 3 shows the electric field distribution of the dielectric compound grating at the resonant wavelength, where γ is -0.05 ($n = 3.4$), -0.15 ($n = 3.3$) and -0.25 ($n = 3.2$). When $\gamma = -0.05$, the electric field energy of the dielectric compound grating is significantly higher than that of $\gamma = -0.15$ and $\gamma = -0.25$. This is because a smaller γ corresponds to a lower degree of asymmetry of the grating, and less energy leaks out through the radiation channels.

In Fig. 2, as the asymmetric parameter γ gradually deviates from 0, the Fano resonance linewidth widens, which decreases the Q factor. Because the Q factor significantly affects the sensor sensitivity and GH shift,[13,14,43] the effect of γ on the Q factor of the dielectric grating QBIC resonance must be studied. Because the QBIC resonance is a Fano-like resonance, we fit the resonance based on the classical Fano formulation. The classical Fano[44] formula is given by

$$T(\omega) = T_0 + A_0 \frac{[q + 2(\omega - \omega_0)/\Gamma]^2}{1 + [2(\omega - \omega_0)/\Gamma]^2}, \tag{4}$$

where ω_0 is the resonant frequency, Γ is the resonant linewidth, T_0 is the background scattering parameter, A_0 is the coupling coefficient between continuous and discrete states and q is the Breit–Wigner–Fano parameter, which determines the asymmetry of the resonant spectral lines. According to Eq. (4), Fano resonances with different material asymmetric parameters can be fitted to obtain $Q = \omega_0/\Gamma$. Figure 3(a) shows the resonance fitting curve of the dielectric compound grating when $\gamma = -0.15$, which is consistent with the simulation results, where $\omega_0 = 1.414 \times 10^{15}$ s^{-1}, $\Gamma = 3.5 \times 10^{11}$ s^{-1} and $Q = \omega_0/\Gamma = 4.04 \times 10^3$.

Based on the above analysis, the Q factor for different material asymmetry parameters γ can be obtained by fitting simulated spectra using Eq. (4), and Fig. 3(b) shows the specific results. In Fig. 3(b), the Q factor of the QBIC resonance rapidly decreases when γ gradually deviates from 0. To obtain a larger Q factor, a smaller γ is favored, but to ensure that the maximum GH shift is located at the reflection peak with perfect reflection, we must consider Fig. 2(a) when determining γ. In Fig. 2(a), when γ is too small, it is difficult for the reflection resonance reflectance to reach 1. Therefore, the minimum value of γ is determined as -0.05 ($n = 3.4$). In this case, the QBIC resonance improves the GH shift and ensures that the maximum GH shift is located exactly at the reflection peak with unity reflectance. The material, whose refractive index is 3.4 near the resonance wavelength, is GaAs (see Fig. 6 for details).

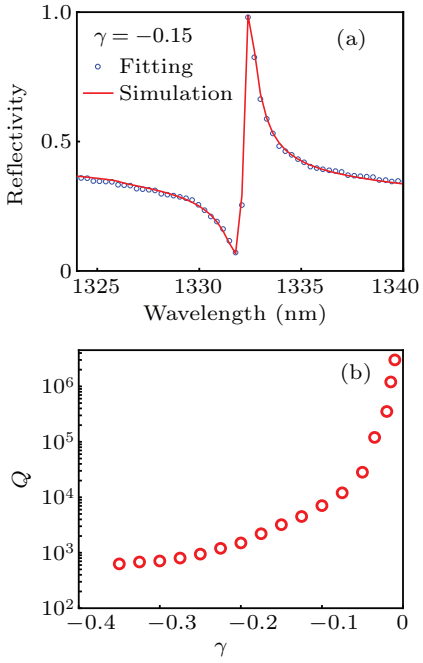


Fig. 4. Fano fitting and the effect of material asymmetry parameter γ on the quality (Q) factor ($w = 200$ nm, $P = 1200$ nm). (a) Results of Fano fitting for $\gamma = -0.15$; (b) effect of γ on Q.

To achieve different Q factors, geometric asymmetric gratings require precise adjustment of the geometric asymmetric parameters, but there may be errors in the fabrication

process, resulting in poor controllability. However, the proposed material asymmetric grating method must only prepare the grating with the required refractive index to achieve the desired Q factor without precisely adjusting the geometrical parameters, which has strong controllability. In the future, the grating with refractive index n could also be replaced with phase-change material[45] or Dirac semimetal,[46] and the dynamic tuning of the Q factor can be realized through current injection or the photothermal effect. This would mean that the required Q factor could be obtained without changing the grating material through semiconductor fabrication technology. This would also be conducive to achieving the dynamic tunability of the GH shift without changing the dielectric compound grating.

3.2. Effect of the grating parameters on the QBIC resonance

In addition to material asymmetry parameter γ, the grating structural parameters affect the QBIC resonance. We calculated the effects of grating width w and grating period P on the dielectric grating reflection spectra, as shown in Fig. 5. In Fig. 5, the QBIC resonance wavelengths are redshifted when w or P increases. The phenomenon can be explained by combining the grating guided-mode resonance and the equivalent medium theory. According to the literature,[15,30,39] the symmetry-protected BIC of the dielectric compound grating proposed in this paper originates from the guided-mode resonance. Because there is dielectric grating, the incident light and waveguide layer can be effectively coupled to cause guided-mode resonance. If the incident light and waveguide layer can be effectively coupled, the wave vector matching condition should satisfy the following conditions:[45]

$$n_{\text{eff}}k_0 = k_x + j\frac{2\pi}{P}, \tag{5}$$

where n_{eff} is the equivalent refractive index of the dielectric compound grating, $k = 2\pi/\lambda_{\text{r}}$ is the incident wave vector, where λ_{r} is the guided-mode resonance wavelength; j is the integer order, and $k_x = k\sin\theta$ is the component of the incident wave vector in the x direction. From Eq. (5), the guided mode resonance wavelength can be deduced as[47]

$$\lambda_{\text{r}} = \frac{(n_{\text{eff}} - \sin\theta)P}{j}. \tag{6}$$

According to Eq. (3), the dielectric compound grating refractive index is the function of w and P. For the convenience of analysis, the influence of w and P on the equivalent refractive index n_{eff} of dielectric gratings will be analyzed using the equivalent medium theory.[39] From the equivalent medium theory,[48] the increase in grating width w will increase the grating equivalent refractive index n_{eff}. According to Eq. (6), the increase in w will redshift the guided-mode resonance wavelength. From the equivalent medium theory, P weakly affects the equivalent refractive index n_{eff} of the dielectric compound grating. However, Eq. (6) shows that P is directly related to the guided-mode resonance wavelength λ_{r}, so an increase in P will inevitably redshift λ_{r}.

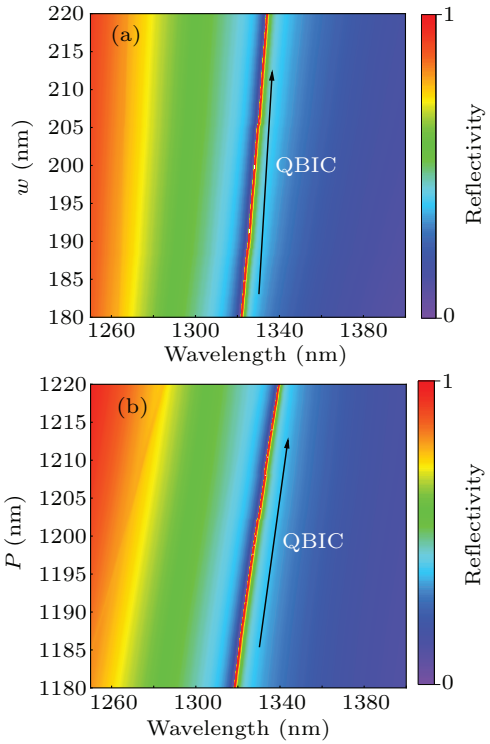


Fig. 5. Effect of the grating parameters on the QBIC resonance ($\theta = 6°$). (a) Grating width ($P = 1200$ nm); (b) grating period ($w = 200$ nm).

3.3. GH shift enhancement

In this section, we use the QBIC resonance excited by material asymmetry to achieve GH shift enhancement ($w = 200$ nm, $P = 1200$ nm). The material asymmetric parameter γ is set at -0.05 ($n = 3.4$), -0.15 ($n = 3.3$) and -0.25 ($n = 3.2$). Figure 2(b) shows that the corresponding QBIC resonance wavelength λ ($\theta = 6°$) of $\gamma = -0.05$, -0.15 and -0.25 are 1335.14 nm, 1332.39 nm and 1330.26 nm, respectively, which correspond to the following three existing materials GaAs, AlSb, InP, respectively. Their refractive indices at resonant wavelengths λ are approximately[49–51] 3.4, 3.3 and 3.2, as shown in Fig. 6. These three materials are common semiconductor materials with mature fabrication and etching technology.

We calculated their reflection angle spectra by fixing the incident wavelength (λ), as shown in Fig. 7. By comparing Fig. 2(b) with Fig. 7, we find that a narrower reflectance spectral linewidth corresponds to a narrower reflectance angle spectral linewidth. In Fig. 7, the resonant wavelength reflectance reaches 1 near $\theta = 6°$. According to the stationary phase method, when the incident light has a sufficiently wide

beam waist, the GH shift can be expressed as[31]

$$D_{\mathrm{GH}} = -\frac{\lambda_0}{2\pi}\frac{\partial\varphi}{\partial\theta}, \tag{7}$$

where φ is the reflection phase. From Eq. (7), the GH shift is proportional to the partial derivative of the reflection phase to the incident angle. Therefore, to obtain the GH shift for different γ values, we calculated the reflection phase angle spectra based on the resonant wavelength, as shown in Fig. 8. When γ decreases from -0.05 to -0.25, the slope of the reflection phase near $\theta = 6^\circ$ gradually decreases.

Based on Eq. (3) and Fig. 8, the GH shifts of different γ values are calculated and shown in Fig. 9. The GH shift can reach $-980\lambda_0$ when $\gamma = -0.05$, but the GH shift is only $-180\lambda_0$ when $\gamma = -0.25$. Therefore, when the dielectric compound grating is composed of Si and GaAs materials, the GH shift is maximized. When γ decreases from -0.05 to -0.25, the GH shift rapidly decreases. This is because when γ is -0.05 and -0.25, the Q factor that corresponds to the dielectric compound grating is approximately 2.8×10^4 and 1×10^3, respectively. The Q factor affects the change in the reflection phase of the dielectric grating near the resonance angle. A larger Q factor corresponds to a more drastic change in the reflection phase.[16–18] Therefore, the GH shift is extremely high when $\gamma = -0.05$, and when $\gamma = -0.25$, the GH shift will sharply decrease.

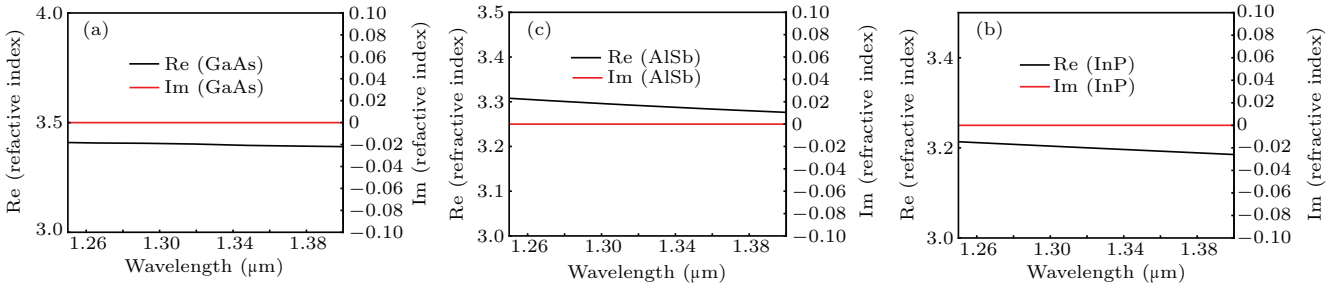


Fig. 6. Refractive indices of GaAs (a); AlSb (b); InP (c) at different wavelengths.

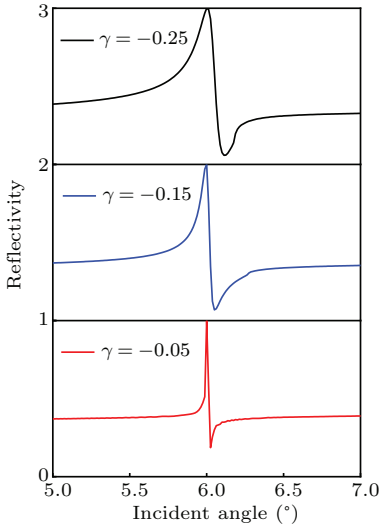


Fig. 7. Reflection angle spectrum for different material asymmetry parameters γ.

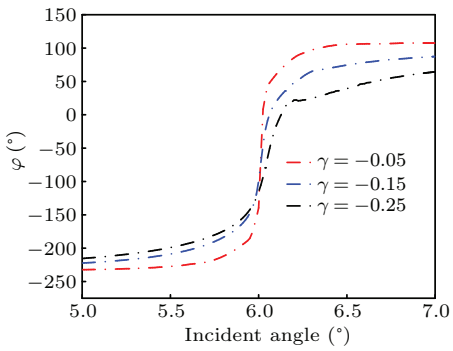


Fig. 8. Reflection phase angle spectrum for different material asymmetry parameters γ.

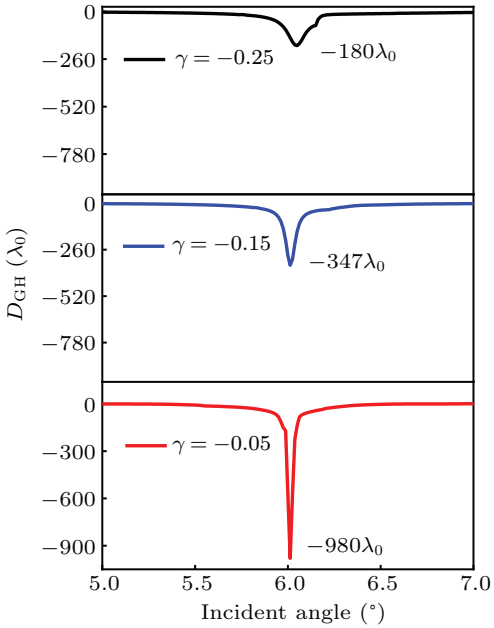


Fig. 9. Goos–Hänchen (GH) shift angle spectrum for different material asymmetry parameters γ.

The guided-mode resonance under oblique incidence is divided into two resonances of ±1 order. This paper studies the $+1$ order resonance, and the propagation constant of the guided mode is negative, which will cause backward propagation resonant guided mode and result in a negative GH shift.[13,14] Currently, there are several studies on improving the positive GH shift based on QBIC,[13,36,37] but there are few studies on enhancing the negative GH shift. Therefore, in this paper, we choose to study the $+1$ order guided-mode

resonance to enhance the negative GH shift.

To explore the effect of the grating structural parameters on the GH shift, we calculated the GH shift for different grating periods P and grating widths w, as shown in Fig. 10 ($\gamma = -0.05$). The GH shift can clearly be tuned by changing P or w, but the effect is not as significant as that of γ because the main factor that affects the Q factor is the material asymmetry parameter γ. When P and w change, the resonance angle that corresponds to the maximum GH shift shifts. When P increases from 1195 nm to 1205 nm, the resonance angle that corresponds to the maximum GH shift shifts from 6.02° to 6°. When w decreases from 205 nm to 195 nm, the resonance angle that corresponds to the maximum GH shift shifts from 6.02° to 6°.

The dielectric compound grating has a high Q factor Fano resonance at $\gamma = -0.05$ ($w = 200$ nm, $P = 1200$ nm), so it can be used as a high-sensitivity refractive index sensor in climate monitoring and biochemical detection. Most refractive index sensors are based on the change in resonance wavelength,[52,53] whereas our sensor is based on the change in GH shift, which will greatly improve the sensor sensitivity. As shown in Fig. 11, when n_{air} increases from 1 to 1.0001, the GH shift changes by 190 μm at $\theta = 6.01°$. The refractive index sensitivity is $S = \Delta D_{GH}/\Delta n_{air} = 1.9 \times 10^6$ μm/RIU, which is significantly higher than those in Refs. [50–54]. However, the sensitivity in Ref. [37] is one order of magnitude higher than ours because the presence of a substrate in our structure introduces an asymmetry in the z-direction, and the symmetry-protected BIC is extremely sensitive to symmetry-breaking perturbations.[55] In reality, to fabricate substrate-free metasurface is truly a challenge.

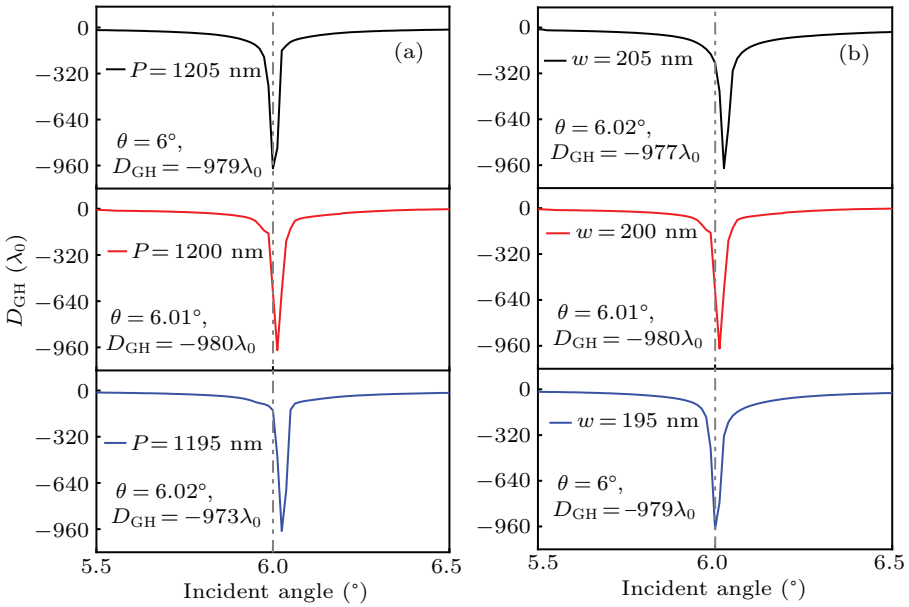


Fig. 10. Effect of grating period P and width w on the Goos–Hänchen shift: (a) P ($w = 200$ nm); (b) w ($P = 1200$ nm).

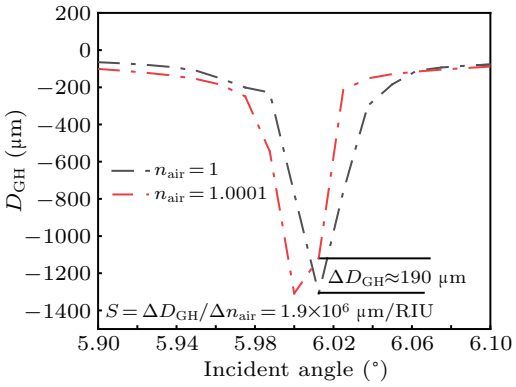


Fig. 11. Effect of the environmental refractive index on the Goos–Hänchen shift of dielectric compound gratings.

4. Conclusion

In this paper, the QBIC resonance with a high Q factor and high reflection was realized by breaking the material symmetry of the dielectric compound grating, and the QBIC resonance was applied to improve the GH shift. The effects of material asymmetry parameter γ and grating structural parameters on the Q factor and resonance wavelength were analyzed based on the finite-difference time-domain method. γ is the key factor that determines the Q factor. When γ decreases, the Q factor will sharply drop. The QBIC resonance wavelength is modulated by the grating width and period, and it will be redshifted when the grating width and period increase. The reflection angle spectra and reflection phase angle spectra of dielectric compound gratings were calculated for $\gamma = -0.05$ ($n = 3.4$), -0.15 ($n = 3.3$) and -0.25 ($n = 3.2$). A smaller material asymmetry parameter corresponds to a narrower reflection angle spectrum and a more drastic change in the reflection phase angle near the resonance angle. The material asymmetry-based QBIC was applied to enhance the GH shift. Based on the stationary phase method, the GH shift can reach

−980 times the resonance wavelength when $\gamma = -0.05$ (n is GaAs material), and the maximum GH shift corresponds to reflectance 1. Finally, using the dielectric grating as a refractive index sensor, the sensitivity of the refractive index sensor can reach 1.9×10^6 μm/RIU.

Acknowledgements

Project supported by the Zhejiang Provincial Natural Science Foundation of China (Grant No. LQ23F040001), the National Natural Science Foundation of China (Grant No. 12204446), the Public Welfare Technology Research Project of Zhejiang Province (Grant No. LGC22E050006), and the Quzhou Science and Technology Project of China (Grant No. 2022K104).

References

[1] Wang W H, Srivastava Y K and Tan T C 2023 *Nat. Commun.* **14** 2811
[2] Li J T, Li J and Zheng C L 2021 *Carbon* **182** 506
[3] Kodigala A, Lepetit T and Gu Q 2017 *Nature* **541** 196
[4] Koshelev K, Kruk S and Melik-Gaykazyan E 2020 *Science* **367** 288
[5] Bernhardt N, Koshelev K and White S 2020 *Nano Lett.* **20** 5309
[6] Hong P L, Xu L and Rahmani M 2022 *Opto-Electronic Adv.* **5** 200097
[7] Bahadori-Haghighi S, Ghayour R and Sheikhi M H 2019 *J. Appl. Phys.* **125** 073104
[8] Sharma S, Lahiri B and Varshney S 2023 *J. Phys. D: Appl. Phys.* **56** 055104
[9] Zhou Y, Guo Z H and Zhao X Y 2022 *Adv. Opt. Mater.* **10** 2200965
[10] Sun K L, Jiang H and Bykov D A 2022 *Photon. Res.* **10** 1575
[11] Shi W Q, Gu J Q and Zhang X Y 2022 *Photon. Res.* **10** 810
[12] Fan J X, Li Z L and Xue Z Q 2023 *Opto-Electronic Sci.* **2** 230006
[13] Wang Z, Liang Y and Qu J Q 2023 *Photon. Res.* **11** 260
[14] Wu F, Wu J J and Guo Z W 2019 *Phys. Rev. Appl.* **12** 014208
[15] Wu F, Ma L and Wu J J 2021 *Phys. Rev. A* **104** 023518
[16] Bulgakov E and Sadreev A 2011 *Phys. Rev. B* **83** 235321
[17] Ma H B, Niu J R and Gao B T 2023 *Adv. Opt. Mater.* **11** 2202584
[18] Song F H, Xiao B G and Qin J Y 2023 *Opt. Express* **31** 4932
[19] Feng G, Chen Z H and Mi X Y 2023 *Opt. Laser Technol.* **164** 109578
[20] Berte R, Weber T and Menezes L D 2023 *Nano Lett.* **23** 2651
[21] Liu J Q, Chen C D, Li X 2023 *Opt. Express* **31** 4347
[22] Yu SH L, Wang Y S and Gao Z A 2022 *Opt. Express* **30** 4084
[23] Chen Y, Li M J and Zhao M 2023 *Opt. Mater.* **138** 113693
[24] Gao E D, Li H J and Liu C H 2022 *Phys. Chem. Chem. Phys.* **24** 20125
[25] Zhang Y, Chen D L and Ma W B 2022 *Opt. Lett.* **47** 5517
[26] Mu Q, Fan F and Ji Y 2019 *Opt. Commun.* **460** 125163
[27] Goos F and Hänchen H 1947 *Ann. Phys.* **436** 333
[28] Wang C L, Wang F Q and Liang R S 2018 *Opt. Mater. Express* **8** 718
[29] Kong W J, Sun Y and Lu Y 2020 *Results Phys.* **17** 103107
[30] Du X D and Da H X 2021 *Opt. Commun.* **483** 126606
[31] Wu H B, Luo Q L and Chen H J 2019 *Phys. Rev. A* **99** 033820
[32] Artmann K 1948 *Ann. Phys.* **437** 87
[33] Zhang C W, Hong Y and Li Z Y 2022 *Appl. Optics* **61** 844
[34] Zoghi M 2020 *Opt. Commun.* **475** 126265
[35] Zheng ZH W, Lu F Y and Jiang L Y 2019 *Opt. Commun.* **452** 272
[36] Wong Y P, Miao Y and Skarda J H 2018 *Opt. Lett.* **43** 2803
[37] Zheng Z Z, Zhu Y and Duan J 2021 *Opt. Express* **29** 29541
[38] Huang Z M, Liu W C and Wei Z C 2023 *Opt. Commun.* **540** 129507
[39] Liu W X, Li Y H and Jiang H T 2013 *Opt. Lett.* **38** 163
[40] Fang C Z, Yang Q Y and Yuan Q C 2021 *Opto-Electron Adv.* **4** 200030
[41] Han S, Pitchappa P and Wang W H 2021 *Adv. Opt. Mater.* **9** 2002001
[42] Chen X and Fan W H 2020 *Nanomaterials* **10** 623
[43] Wang M and Wang W D 2023 *Euro. Phys. J. D* **77** 57
[44] Li H, Yu S and Yang L 2021 *Opt. Laser Technol.* **140** 107072
[45] Kim Y H, Wu P C and Sokhoyan R 2019 *Nano Lett.* **19** 3961
[46] Gao J X, Liu H and Zhang M 2022 *Phys. Chem. Chem. Phys.* **24** 25571
[47] Chen Y, Li M J and Zhang M 2023 *Phys. Scr.* **98** 025505
[48] Zhu J C, Zhou J K and Shen W M 2019 *Electron. Lett.* **55** 756
[49] Papatryfonos K, Angelova T and Brimont A 2021 *AIP Adv.* **11** 025327
[50] Djurisic A B, Li E H and Rakic D 2000 *Appl. Phys. A* **70** 29
[51] Adachi S 1990 *J. Appl. Phys.* **67** 6427
[52] Feng G, Chen Z H and Wang Y 2023 *Chin. Opt. Lett.* **21** 031202
[53] Abbas M A, Zubair A and Riaz K 2020 *Opt. Express* **28** 23509
[54] Ruan Y H, Hu Z D and Wang J C 2022 *IEEE Photonics J.* **14** 4655906
[55] Fang C Z, Yang Q Y and Yuan Q C 2021 *Opto-Electron. Adv.* **4** 200030